

# Assessment of Gamma-Ray Spectrum Transmission with Scintillator Shading Variations for Determining Minimal Transmission Diameter

Tadeas Zbozinek<sup>1,2,\*</sup>, Michal Jelinek<sup>1</sup>, and Bretislav Mikel<sup>1</sup>

<sup>1</sup>Institute of Scientific Instruments of the CAS, v. v. i., The Czech Republic

<sup>2</sup>Department of Microelectronics FEEC BUT, The Czech Republic

(\*) [zbozinek@isibrno.cz](mailto:zbozinek@isibrno.cz)

**Abstract—** Gamma-ray spectroscopy is essential for identifying radioactive sources, but direct coupling of scintillators to photodetectors risks exposing sensitive electronics to radiation damage in high-radiation environments. Optical fibres offer a safer alternative by transmitting scintillation light over long distances, although differences in diameter can reduce spectral resolution for larger crystals, making precise spectroscopy difficult. To address this issue, we introduce an experimental setup that uses an adjustable iris and aperture plate to simulate fibre cores of various diameters, paired with scintillators of different sizes. We systematically measured the transmitted light intensity and spectral peak resolution at each aperture setting to analyse the relationship between core diameter, scintillator size, and spectral resolution. By optimising the balance between scintillator size and effective aperture, we can retain the advantages of larger crystals, enabling spectral analysis with smaller detection diameters. This work offers practical guidelines for selecting optimal configurations of detector and scintillator sizes, which are essential for monitoring gamma radiation with an optimal balance of high resolution and sufficient sensitivity.

**Keywords —** Scintillation, Aperture, ionising radiation, optical fibre,

## I. INTRODUCTION

THE utilisation of ionising radiation encompasses a wide range of applications. As radiation is hazardous, facilities, including nuclear plants, require a stable monitoring system to measure personnel dose continuously. Standard methods, like ionising chambers, semiconductors and scintillators, provide sufficiently precise measurements. Difficulties occur in sites with higher radiation dose rates, experimental sites and spatially limited areas. These areas face measurement challenges due to electronic interference, size and access limitations, and radiation-induced damage [1]. The effects that influence the evaluation, particularly the damage caused by radiation, can ultimately shorten the lifespan of the equipment [2,3]. An optical fibre can be introduced into the measurement system

to overcome these restrictions, maintaining distance from radiation sources and enabling access to confined spaces.

Several methods utilising optical fibres are used in the field of radiation measurement. Absorption techniques take advantage of changes in optical fibre attenuation during radiation exposure [4,5]. The Bragg grating technique observes wavelength shifts in gratings incorporated into fibres [4,6]. However, from the perspective of this paper, the most interesting method lies in luminescence-based detection, specifically radiation-induced luminescence: scintillation.

Plastic fibres are often used within these techniques, as they provide an efficient, easier-to-manufacture, and more cost-effective way to measure radiation. To preserve radiation sensing, enhance resistance, and create a probe-type device, the scintillation material should not be doped into the fibre but used as a separate crystal mounted at the fibre's end [7,9]. This approach ensures good linear counting properties, flexibility in scintillator material and shape choice, radiation resistance, and the ability to measure over longer distances [9]. In this field, several probes were tested using plastic fibres, which are easily manufactured in larger diameters and allow larger scintillators to be used [10 – 15].

However, from a radiation resistance perspective, the optical properties of plastic fibres are less resistant to radiation damage than those of silica or fluoride-doped silica fibres [9,16,17,18]. The silica optical fibres can also be used for counting with theoretically better transportation and radiation resistance properties, but are commercially restricted to a diameter of 1 – 1.5 mm [9,19].

We focus on adding an appropriate scintillator material and adjusting its volume; this work can enhance the detection system's efficiency and sensitivity. However, an undesirable effect has been observed in our design: the signal from the scintillator is impacted by diameter mismatches at the fibre-scintillator interface, resulting in degraded optical fibre transmission. Therefore, the pulse shape is altered, quickly reducing energy resolution and making spectral analysis impossible.

Measurement is proposed to address issues related to the silica fibre's dimensional limitations and to clarify

the relationship between scintillator size and fibre diameter. Replacing an optical fibre with a shading aperture allows us to adjust the proportion of light reaching the detector. Gradual shading enables us to observe changes in the gamma spectrum and identify transmission limits. This approach provides an approximated simulation of the varying light fraction from the scintillator necessary for transmitting a resolvable gamma spectrum, from which the appropriate optical fibre diameter can be determined. Consequently, the successful characterisation of the mentioned measurement allows us better to understand the behaviour of the optical fibre setup, guiding us in a more effective design of our fibre-based measurements.

## II. METHODOLOGY

Our previously presented work's high-radiation-resistance real-time monitoring system combines optical fibres with a scintillator crystal [9]. We use large-diameter (1 and 1.5 mm) silica multimode, step-index polished fibres FP1500URT (supplied by Thorlabs) to maximise light collection at the scintillator side (Fig. 1). Yet these large multimode fibres exhibit high modal dispersion, distorting the scintillation pulse. Only a fraction of each pulse is collected, and transporting that small signal through the fibre further limits the pulse shape. Although a high numerical aperture (NA) improves collection efficiency, it also increases modal dispersion and broadens pulses. With a small collection diameter and significant modal dispersion, achieving the required level of gamma-spectrum resolution and pulse discrimination is difficult. Initially, we focused on the fraction of light collected by the optical fibre and pulse amplitude, as preserving amplitude is essential for gamma spectroscopy.

By replacing the optical fibre with an iris of similar diameter, we can simulate its effect on light collection and predict system behaviour. We measured relative light collection (i.e., the fraction of scintillator light captured) by varying the iris opening. The iris was replaced with sets of shading apertures to obtain more precise results and adapt the measurement for differently sized crystals. This adjustment allows for replicating the measurement and decreases the distance between the crystal and the photocathode of the photomultipliers, which was created due to the iris dimensions. It is worth noting that both shading methods simulate optical fibre only partially, as their numerical aperture approaches 1. In contrast, optical fibre is limited by material properties, achieving NA 0.5 with current fibres in use. Still, we can determine how many photons we need from the scintillators for the spectrum resolution.

## III. EXPERIMENTAL MEASUREMENT

To study the shading effect, we measured three NaI(Tl) crystals to ensure that proportionality holds across different sizes. A common 2" in diameter NaI(Tl) was first tested with an iris; then smaller 1"x2" and 1"x1" cylinders were tested using a shading aperture, alongside the large one again for consistency. All measurements used a  $^{137}\text{Cs}$  source to define the gamma spectrum clearly due to its single peak at 662 keV.

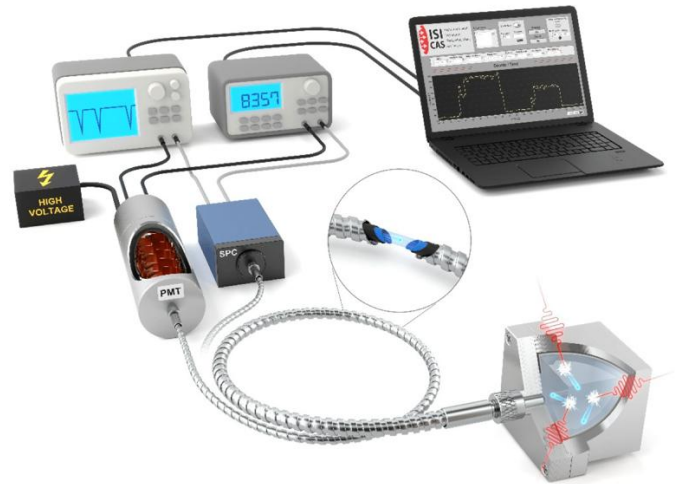


Fig. 1: Measurement of ionizing radiation activity with an optical fibre [9]

### A. Experimental setup

The setup comprised Saint-Gobain NaI(Tl) scintillators, an iris or shading aperture, and an ET Enterprises 9266KB photomultiplier tube. The PMT output went directly into a CAEN DT5751 digitiser for pulse-amplitude recording and spectrum evaluation. Experiments with the iris suffered from an excessive distance between the scintillator and PMT, so a shading aperture was introduced to minimise the gap to 0.1 mm. The experiment was enclosed in a light-tight black box to eliminate ambient-light interference. Schematic measurement is illustrated in Figure 2.

### B. Measurement

Each spectrum was recorded with a ten-minute counting interval to ensure adequate statistics. Initially, the 2" crystal was placed next to the iris adjacent to the PMT, then the iris diameter was gradually decreased, and measurements were taken at each setting. The diameter was reduced in 5 mm steps, except for the first step due to iris size limitations, resulting in the sequence (48, 45, 40, 35, 30, 25, 20, 15) mm. Next, to compensate for the spectrum shift caused by shading, the PMT gain was increased so that the photopeak is positioned on the same digitiser channel, facilitating direct comparison. Finally, the procedure was repeated for all three crystals using shading apertures whose hole diameters were scaled relative to each crystal's face area.

### C. Evaluation

After all measurement series were completed, each series was evaluated separately. For the large 2" NaI(Tl), we determined the smallest surface/diameter at which

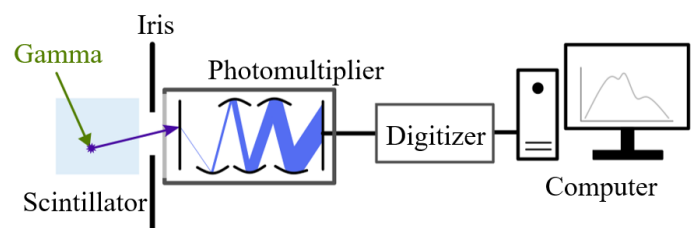


Fig. 2: Schematic illustration of the experiment

the photopeak remained recognisable and the individual parts of the gamma spectrum (the Compton continuum and Compton edge) were still separable. These results were then used to set the minimum aperture diameter for subsequent measurements and to calculate the resolution for each crystal size. Finally, all crystals were compared to illustrate the relationship between crystal size and required aperture diameter.

#### IV. RESULTS DISCUSSION

In the first measurement, we used an iris with a decreasing diameter. As the aperture closed and the shaded area increased, the number of photons reaching the detector decreased, causing the photopeak channel in the gamma spectrum to shift lower (channel number is proportional to collected photon count). The resulting graph is shown in Fig. 3. With this setup, we could transmit the spectrum with a 35 mm diameter (47% of surface area). By adjusting the PMT gain, the minimum

aperture diameter at which parts of the spectrum remained visible was 15 mm (9 % of scintillator surface), with a resolution of 19,6 %. With further reductions in aperture diameter, the spectrum becomes dominated by noise and barely readable, making it difficult to resolve even a single peak, let alone multiple ones. This is why we observe a minimal transmission diameter corresponding to 15 mm iris diameter (9% of the original surface area).

After these observations, all three crystal sizes were measured under the same conditions, with resulting spectra plotted in Fig. 6, which shows the same trend for all sizes. The resolutions with corresponding diameters are summarised in Table 1 and shown graphically in Fig. 5. A direct comparison of all measured diameters is provided with the corresponding photopeak resolutions.

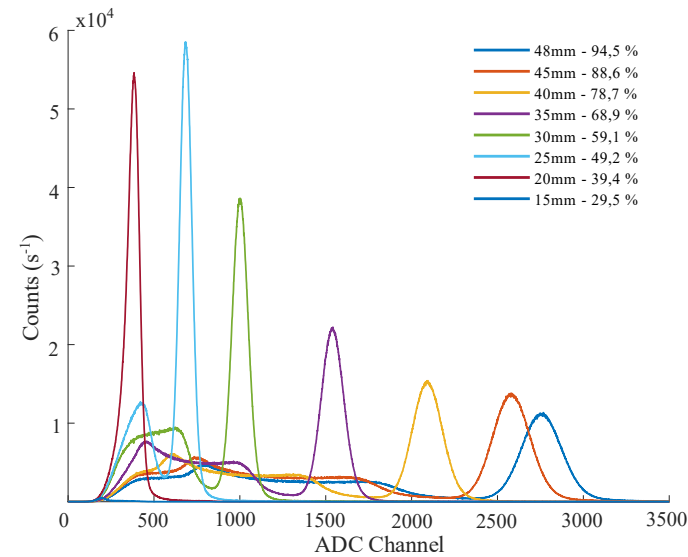


Fig. 3: The energy spectra of gamma radiation obtained by shading the scintillation detector NaI(Tl); each curve corresponds to the spectrum of a specific opening of the iris (Caesium 137) [20]

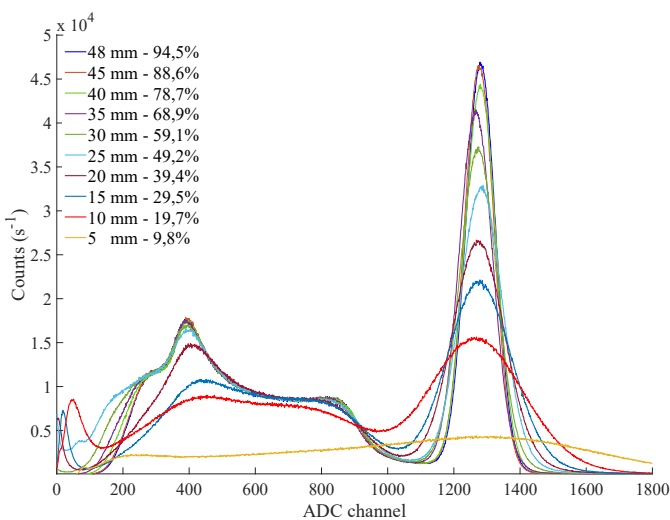


Fig. 4: Gamma-ray energy spectra (137Cs) obtained by shielding the NaI(Tl) scintillation detector - Gradual increase of the photomultiplier gain to align the peak positions [20]

TABLE 1

COMPARISON OF APERTURE DIAMETER (EXPOSED SURFACE TO PMT) AND CALCULATED RESOLUTION FOR DIFFERENT SIZES OF CRYSTALS

Scintillator size					
2"x 2"		1"x 2"		1"x 1"	
∅ (mm)	Res. (%)	∅ (mm)	Res. (%)	∅ (mm)	Res. (%)
15.0	19.6	7.0	23.5	7.0	29.2
20.0	16.8	10.0	19.6	10.0	25.8
25.0	15.7	12.5	17.6	12.5	24.6
30.0	14.5	15.0	17.4	15.0	22.4
35.0	14.0	18.0	15.0	18.0	22.5
40.0	13.5	20.0	14.2	20.0	21.4
45.0	13.1	22.0	13.8	22.0	21.8
48.0	13.1	24.0	13.8	24.0	21.3

The minimum resolvable resolution for symmetrically shaped crystals at 9 % scintillator area is 19.6 %. Symmetrical scintillators maintain the same spectral shape and resolution; only the channel numbers differ (due to different sizes). For the elongated crystal (1"x2"), a resolution of 23.5 % at 9%

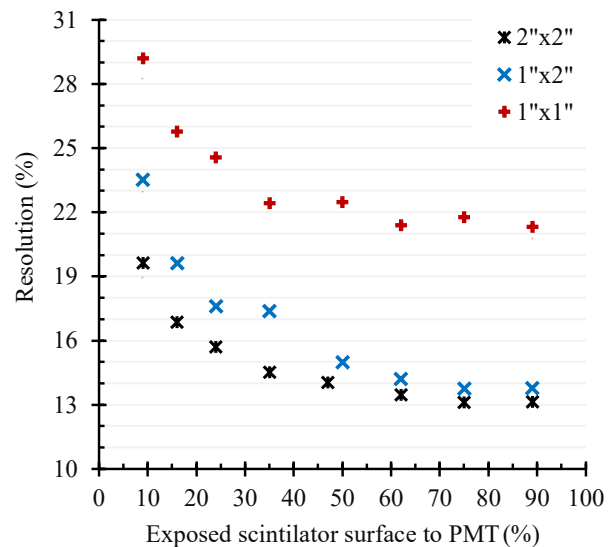


Fig. 5: Comparison of the variation in energy resolution during shading for scintillation crystals of three different sizes

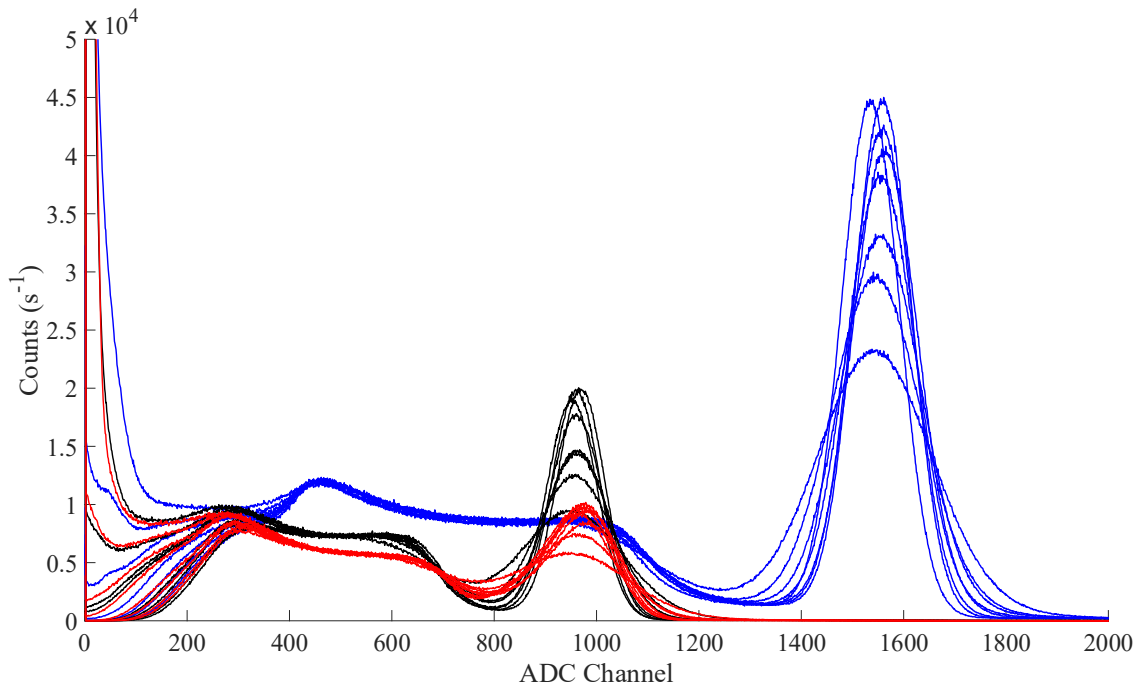


Fig. 6: Gamma-ray energy spectra ( $^{137}\text{Cs}$ ) obtained by shielding three differently sized NaI(Tl) scintillation crystals - Gradual increase of the photomultiplier gain to align the peak positions for each crystal. Sizes: 2" x 2" (blue), 1" x 2" (black) and 1" x 1" (red).

scintillator area was observed, likely because its geometry is better suited for capturing gamma photons along the crystal's long axis, in which the etalon was placed (in comparison to 1" x 1" scintillator, where resolution is 29.2 %). This approach preserves the advantages of a larger crystal while allowing gamma spectrum evaluation even with reduced resolution due to the smaller collector diameter, thus demonstrating that spectral transmission remains possible even when connected to much smaller optical fibres.

## V. CONCLUSION

Three NaI(Tl) scintillators of different sizes were gradually shaded and the resulting gamma spectra analysed. The progressive reduction of the aperture diameter (the fraction of scintillation light captured) produced similar behaviour across all crystal sizes. Resolution remains relatively stable until more than 50% of the scintillator face is shaded, beyond which it increases rapidly; spectral features and resolution exhibit the same tendency. To transmit a recognisable spectrum from a cylindrically symmetric NaI(Tl) crystal, at least 9% of the crystal face must remain exposed. Resolutions achieved were 19.6% for the 2" crystal, 23.5% for the 1" x 2" crystal, and 29.2% for the 1" x 1" crystal. Further reductions in the exposed area introduce excessive noise and render the spectrum unreadable.

These findings support a new approach to scintillator-fibre dosimetry with full gamma-spectrum resolution. By clarifying the relationship between fibre properties and scintillator geometry, crystal size can be optimised to maximise count rate and increase efficiency, enabling compact and flexible detector designs. The results suggest that, for fibre transfer, a small crystal with asymmetric dimensions is required to achieve spectral transmission. This opens the way for flexible and

robust gamma-ray spectroscopy in high-dose, spatially constrained, and hard-to-access environments.

## REFERENCES

- [1] G. F. Knoll, *Radiation detection and measurement*, 4th ed. Hoboken: Wiley, c2010.
- [2] E. Garutti and Y. Musienko, "Radiation damage of SiPMs", *Nuclear Instruments and Methods in Physics Research Section A: Accelerators, Spectrometers, Detectors and Associated Equipment*, vol. 926, 2019, doi: 10.1016/j.nima.2018.10.191.
- [3] V. A. J. Van Lint, "The physics of radiation damage in particle detectors", *Nuclear Instruments and Methods in Physics Research Section A: Accelerators, Spectrometers, Detectors and Associated Equipment*, vol. 253, no. 3, 1987, doi: 10.1016/0168-9002(87)90532-8.
- [4] S. O'Keefe *et al.*, "A review of recent advances in optical fibre sensors for in vivo dosimetry during radiotherapy", *The British Journal of Radiology*, vol. 88, no. 1050, 2015, doi: 10.1259/bjr.20140702.
- [5] J. Hou, Z. Feng, G. Ma, W. Zhang, Z. Meng, and Y. Li, "Research on the Intrinsic Sensing Performance of an Optical Fiber Dosimeter Based on Radiation-Induced Attenuation", *Sensors*, vol. 25, no. 12, Jun. 2025, doi: 10.3390/s25123716.
- [6] K. Krebber, H. Henschel, and U. Weinand, "Fibre Bragg gratings as high dose radiation sensors?", *Measurement Science and Technology*, vol. 17, no. 5, Apr. 2006, doi: 10.1088/0957-0233/17/5/s26.
- [7] E. Lewis *et al.*, "Terbium-doped gadolinium oxysulfide (Gd<sub>2</sub>O<sub>2</sub>S:Tb) scintillation-based polymer optical fibre sensor for real time monitoring of radiation dose in oncology", in *SPIE Proceedings*, SPIE, May 2014. doi: 10.1117/12.2058572.
- [8] D. McCarthy *et al.*, "Radiation Dosimeter Using an Extrinsic Fiber Optic Sensor", *IEEE Sensors Journal*, vol. 14, no. 3, 2014, doi: 10.1109/jсен.2013.2284857.
- [9] M. Jelinek, O. Cip, J. Lazar, and B. Mikel, "Design and Characterisation of an Optical Fibre Dosimeter Based on Silica Optical Fibre and Scintillation Crystal", *Sensors*, vol. 22, no. 19, Sep. 2022, doi: 10.3390/s22197312.
- [10] D. Dohler, L. Alshut, L. Konig, T. Teichmann, T. Werner, and T. Kormoll, "Characterization of a Fiber Optic Radiation Sensor Prototype for Nuclear Dismantling", *IEEE Transactions on Nuclear Science*, vol. 69, no. 8, 2022, doi: 10.1109/tns.2022.3189787.

- [11] S. Yamamoto, I. Aoki, and T. Higashi, “Optical fiber-based ZnS(Ag) detector for selectively detecting alpha particles”, *Applied Radiation and Isotopes*, vol. 169, 2021, doi: 10.1016/j.apradiso.2020.109495.
- [12] W. Yoo, S. Shin, D. Lee, K. Jang, S. Cho, and B. Lee, “Development of a Small-Sized, Flexible, and Insertable Fiber-Optic Radiation Sensor for Gamma-Ray Spectroscopy”, *Sensors*, vol. 15, no. 9, Aug. 2015, doi: 10.3390/s150921265.
- [13] K. Watanabe, “Applications of scintillators in optical-fiber-based detectors”, *Japanese Journal of Applied Physics*, vol. 62, no. 1, Nov. 2022, doi: 10.35848/1347-4065/ac90a5.
- [14] L. Ding, Q. Wu, Q. Wang, Y. Li, R. M. Perks, and L. Zhao, “Advances on inorganic scintillator-based optic fiber dosimeters”, *EJNMMI Physics*, vol. 7, no. 1, Oct. 2020, doi: 10.1186/s40658-020-00327-6.
- [15] J. H. Kim *et al.*, “Gamma-ray Spectroscopy Using Inorganic Scintillator Coated with Reduced Graphene Oxide in Fiber-Optic Radiation Sensor”, *Photonics*, vol. 8, no. 12, Nov. 2021, doi: 10.3390/photonics8120543.
- [16] J. Li *et al.*, “Radiation Damage Mechanisms and Research Status of Radiation-Resistant Optical Fibers: A Review”, *Sensors*, vol. 24, no. 10, May 2024, doi: 10.3390/s24103235.
- [17] S. Girard *et al.*, “Radiation Effects on Silica-Based Optical Fibers: Recent Advances and Future Challenges”, *IEEE Transactions on Nuclear Science*, vol. 60, no. 3, 2013, doi: 10.1109/tns.2012.2235464.
- [18] M. Kovacevic *et al.*, “Measurement of  $^{60}\text{Co}$  gamma radiation induced attenuation in multimode step-index POF at 530 nm”, *Nuclear Technology and Radiation Protection*, vol. 28, no. 2, 2013, doi: 10.2298/ntrp1302158k.
- [19] S. Kodama *et al.*, “Fiber-read radiation monitoring system using an optical fiber and red-emitting scintillator for ultra-high-dose conditions”, *Applied Physics Express*, vol. 13, no. 4, Mar. 2020, doi: 10.35848/1882-0786/ab77f7.
- [20] T. Zbožinek, M. Jelinek, and B. Mikel, “Evaluation of the gamma-ray spectrum transmitted upon alteration in scintillator shading”, in *Proceedings II of the 30st Conference STUDENT EEICT 2024: Selected papers*, Brno: Brno University of Technology, Faculty of Electrical Engineering and Communication, 2024, pp. 197-201. doi: 10.13164/eeict.2024.197.